Product Yields and Compositions in the Continuous Pyrolysis of High-Density Polyethylene in a Conical Spouted Bed Reactor

ARTICLE *in* INDUSTRIAL & ENGINEERING CHEMISTRY RESEARCH · JUNE 2011

Impact Factor: 2.59 · DOI: 10.1021/ie200186m

I&EC research
Industrial & Engineering Chemistry Research

ARTICLE

pubs.acs.org/IECR

Product Yields and Compositions in the Continuous Pyrolysis of High-Density Polyethylene in a Conical Spouted Bed Reactor

Gorka Elordi,* Martin Olazar, Gartzen Lopez, Maite Artetxe, and Javier Bilbao

Department of Chemical Engineering (Group of Catalytic Processes and Residue Valorization), University of the Basque Country, P.O. Box 644, E48080 Bilbao, Spain

ABSTRACT: The pyrolysis of high-density polyethylene (HDPE) has been carried out in the range between 500 and 700 °C in continuous mode in a pilot-plant unit equipped with a conical spouted bed reactor. The products have been grouped into the lumps of gas (C_{4-}), gasoline (C_5-C_{11}), diesel ($C_{12}-C_{20}$), and waxes (C_{21+}). The product yields and compositions of these fractions were compared both to those previously obtained in the pyrolysis performed in discontinuous mode and to those obtained by other authors in fluidized bed reactors. The results confirm the optimal performance of the conical spouted bed reactor (CSBR) in obtaining high yields of waxes and fuels with low aromatic content, which is explained by the appropriate conditions of the CSBR needed to enhance heat and mass transfer between phases (capacity for coating the sand with plastic) and minimize secondary reactions (short residence time of the volatiles).

1. INTRODUCTION

The pyrolysis (or thermal cracking in an inert atmosphere) of waste plastics, particularly polyolefins, arouses great interest for the valorization of these wastes, as it allows high yields of fuels and raw materials to be obtained for the benefit of the petrochemical industry. Moreover, the pyrolysis process has few environmental issues.[1−5]

The thermal pyrolysis of polyolefins takes place through a complex free-radical mechanism,[6] giving rise to a wide product distribution that depends on the pyrolysis conditions, namely, heating rate, temperature, and residence time.[7−9] The use of acid catalysts, either in situ in the pyrolysis reactor[10−12] or online in the reforming of pyrolysis volatile products,[13,14] improves the quality of the product stream and decreases the required temperature for pyrolysis. Nevertheless, these strategies involve an increase in the costs of capital and catalyst regeneration, which points to the need to continue exploring the possibilities of catalyst-free pyrolysis, especially when it is possible to operate at low temperatures, given that an increase in temperature has a significant impact on the cost of the energy for heating the inert gas.

The selection of a reactor is a key factor for the kinetics of pyrolysis, as well as for the product distribution obtained, which is explained by the fact that the following steps take place from the moment that the waste plastic particles are fed into the reactor (Figure 1): (i) fusion of the plastic and (ii) pyrolysis of the fused plastic. The design of the reactor, with a continuous feeding system, must permit the fast fusion of the plastic in order for pyrolysis (the second step) to be the controlling one. Della Zassa et al.[15] emphasized the importance of isolating the two steps, as shown in Figure 1, to minimize the formation of secondary products, whether gases (methane), liquids [polyaromatic hydrocarbons (PAHs)], or solids (char). Working under these conditions, the yields of products of commercial interest may be optimized by selecting appropriate pyrolysis conditions.

Attempts have been made to improve the fusion step of the plastic fed into the reactor by using different reactors,[16] including screw reactors,[17−20] fluidized beds,[21−30] and spouted beds.[31−34] In these reactors, solid material particles are used (sand or catalyst), which are coated with the fused plastic, facilitating heat and mass transfer between the plastic and the gas. Among the advantages of the conical spouted bed reactor (CSBR) are the following: (i) The cyclic movement of the particles is suitable for fast and uniform coating of the sand or catalyst particles with the fused plastic, improving heat and mass transfer between phases. This movement is characteristic of spouted beds, whose use for the coating of several materials has been widely reported.[35] Similarly, the coating of a solid (catalyst) with a sticky polymer occurs in heterogeneous catalytic polymerization.[36−37] (ii) The movement of the solid particles is more vigorous than that occurring in bubbling fluidized bed reactors, and this minimizes the defluidization problems of the sand particles coated with fused plastic, which is a limitation many authors have observed for fluidized bed reactors.[22,23,29,38] (iii) The short residence time of the volatiles (in the range of centiseconds)[39,40] minimizes the formation of secondary products.

In this work, the yields and compositions of the products were studied in the pyrolysis of high-density polyethylene (HDPE) carried out in continuous mode in a CSBR. Previous studies have reported good performance for this type of reactor in the pyrolysis of polyolefins in discontinuous mode for obtaining the kinetic equation;[31] maximizing the yield of waxes;[32] and incorporating acidic catalysts in situ, which is feasible without segregation problems.[41,42]

2. EXPERIMENTAL SECTION

2.1. Equipment and Pyrolysis Conditions. The HDPE was provided by The Dow Chemical Company (Tarragona, Spain) in the form of 4 mm chippings, with the following properties: average

Received: January 26, 2011
Accepted: April 7, 2011
Revised: April 5, 2011
Published: April 07, 2011

dx.doi.org/10.1021/ie200186m | *Ind. Eng. Chem. Res.* 2011, 50, 6650–6659

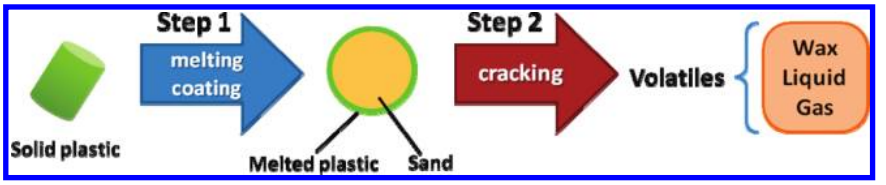

Figure 1. Melting and cracking steps in the pyrolysis of polyolefins.

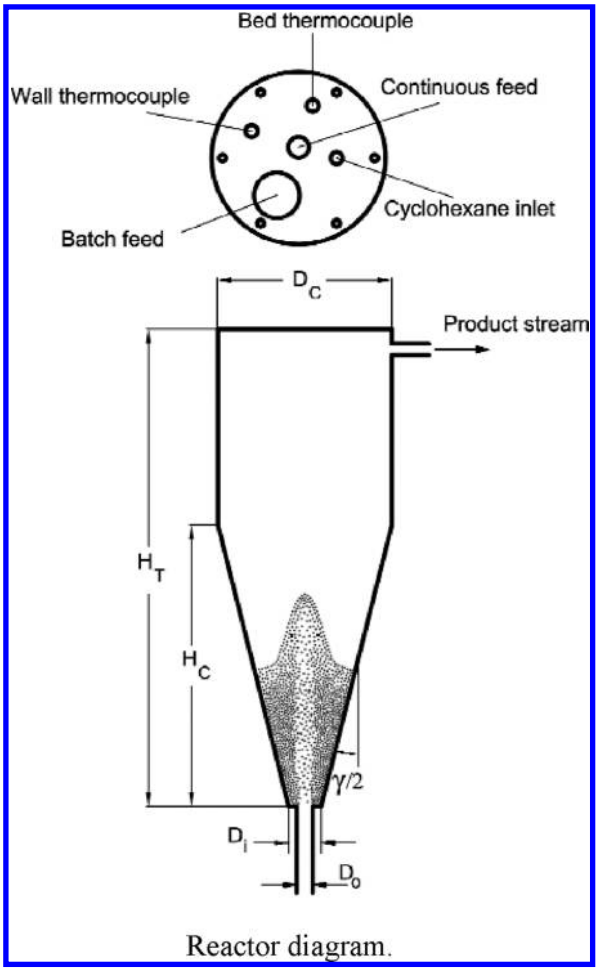

Figure 2. Reactor diagram.

molecular weight, 46.2 kg mol^{-1}; polydispersity, 2.89; density, 940 kg m^{-3}; higher heating value, 43 MJ kg^{-1}. The pyrolysis pilot plant has previously been described.[33,34] The system for feeding the HDPE (chippings) involved a hopper (2 L) with an eccentric vibrator and a three-way hollow ball valve connected to a 0.5-in. pipe cooled by tap water. The device was actuated by an automaton that programmed the frequency for a Swagelok pneumatic actuator.

The N_2 heating system consisted of a cylindrical stainless steel encasing that was 470 mm in length and 38 mm in diameter, with glass-wool external insulation. It was made up of a ceramic cartridge equipped with a resistance that generated 1500 W to heat the gas to the reaction temperature, which was measured with a thermocouple placed above the resistance (below the reactor inlet nozzle). A temperature limit (700 °C) was established, at which the electric supply was cut to avoid the deterioration of the resistance.

The spouted bed reactor, 3 L in volume, was conical in shape with a cylindrical section in the upper part for the development of a fountain (Figure 2). The total height of the reactor, H_T, was 34.00 cm, with a conical section height, H_c, of 20.05 cm and a conical zone angle, γ, of 28°. The diameter of the cylindrical section, D_c, was 12.30 cm; the diameter of the base, D_i, was 2.00 cm; and the diameter of the gas inlet, D_o, was 1.00 cm. These dimensions guarantee bed stability in a wide range of process conditions and were established in previous hydrodynamic studies of conical spouted beds for different materials.[43−51]

Two thermocouples were located inside the reactor, one in the bed annulus and the other close to the wall. The reactor also had a pressure gauge for measuring total and differential pressures, to allow the detection of any increase in pressure drop due to the plugging of gas filters, so that such filters could be replaced. In the reactor lid, near the outlet for the volatile stream, was an inlet for cyclohexane, which was fed as an inert standard compound to close the mass balance together with the results of the gas chromatograph. The outlet pipe for the volatile stream was located perpendicular to the reactor axis.

The condensation system for the volatile stream consisted of (i) a stainless-steel condenser cooled by an antifreeze mixture, which allowed the temperature to be decreased to −10 °C, and (ii) two coalescence filters (made of epoxy ester) that were used to retain over 99.5% of aerosol particles larger than 0.1 μm.

Pyrolysis was carried out in the 500−700 °C range with an HDPE flow rate of 1 g min^{-1}. Below 500 °C, the pyrolysis process is very slow, and consequently, bed defluidization occurs because of the agglomeration of sticky particles.

Based on the results obtained using different amounts of sand in the bed, a quantity of 30 g of sand with a particle diameter in the 0.6−1.2-mm range was determined as the most suitable bed. These values were obtained as a compromise between different factors related to (i) particle momentum (bed turbulence to avoid defluidization), (ii) the rate of coating the particles with fused plastic, and (iii) the inert gas (N_2) flow rate required.

2.2. Product Analysis. The online analysis of the outlet volatile stream (except the waxes) (very diluted in N_2) was carried out by periodically sending samples to a gas chromatograph (Agilent 6890) provided with a flame ionization detector (FID). The following temperature program was used: (i) 4.5 min at 35 °C, to obtain a good separation of C_1−C_4 hydrocarbons; (ii) ramp of 15 °C min^{-1} to 305 °C; and (iii) 5.5 min at 305 °C to ensure that all hydrocarbons were eluted from the HP-PONA column. The yield of each compound was calculated from the ratio between the corresponding mass flow rate and the total mass flow rate of the stream (all volatiles including waxes). This calculation involved monitoring the mass flow rates for all of the volatile components, except the waxes, which were periodically measured by weighing the coalescence filters.

To validate the mass balance, cyclohexane (0.1 mL min^{-1}) was used as an internal standard. This component was fed from the lid into the upper part of the reactor (Figure 2), where it was

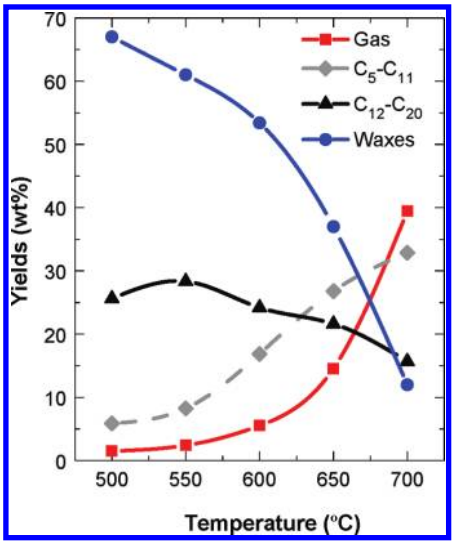

Figure 3. Effect of temperature on the yields of product fractions (wt %). Continuous operation.

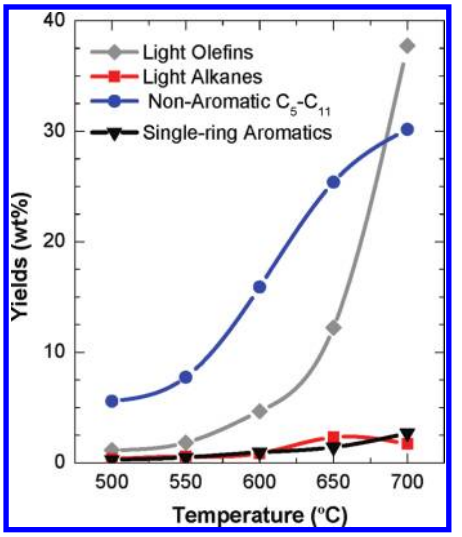

Figure 4. Effect of temperature on the yields (wt %) of the product families of the gas and gasoline fractions. Continuous regime.

incorporated into the outlet product stream. The temperature in this zone was below 400 °C, even at the highest temperature used in the pyrolysis runs (700 °C). Moreover, the outlet stream was very diluted in N_2, and the residence time in this zone for the outlet of volatile products was very short. Consequently, cyclohexane was not cracked, as was verified experimentally. The cyclohexane flow rate in the outlet stream was determined to be the same as that in the inlet by chromatographic analysis.

A gas chromatography/mass spectrometry system (GC/MS; Agilent 3000 micro gas chromatograph and Agilent 5975B inert MSD mass spectrometer) was used to check the absence of hydrogen, carbon monoxide, and carbon dioxide; to determine the ethane/ethylene and propane/propylene ratios more accurately; and to identify the lightest components (with molecular weights lower than 100 g mol^{-1}).

Identification of the components of the liquid fraction (obtained by condensation of the volatile fraction) and waxes (diluted in tetrahydrofuran at 55 °C) was carried out by means of a gas chromatograph coupled with a mass spectrometer (Shimadzu QP2010S). A DB-1MS column of 60-m length, 0.27-mm inner diameter, and 0.25-μm thickness was used in the gas chromatograph. This column was used to separate the products according to their molecular weights. The temperature sequence of the chromatograph oven had the following steps: (i) 40 °C for 2 min, (ii) ramp of 4 °C min^{-1} to 300 °C, (iii) 300 °C for 6 min. The chromatographic analysis conditions were as follows: detected mass interval, 40−400; solvent delay, 4.5 min; injector pressure, 100.3 kPa; total flow rate, 93.2 mL min^{-1}; column flow rate, 0.89 mL min^{-1}, carrier-gas linear velocity, 24.1 cm s^{-1}; split, 1000:1 (although it was reduced in certain cases to increase the peak resolution of the less abundant components).

The simulated distillation of the condensed liquids and waxes were developed according to the ASTM D2887-04 standard, with an Agilent 6890 gas chromatograph provided with an FID detector and a SimDis 2887 fast (10 m × 0.53 mm × 0.88 μm) column.

The waxes were also analyzed by means of high-resolution liquid chromatography (HP 1100 instrument provided with a Tosoh-Haas TSK-GEL GMHHR-M column, 30 cm × 7.8 mm). The equipment was calibrated with polystyrene as the internal standard of different molecular weights and narrow distributions diluted in tetrahydrofuran, with toluene as a marker. The nature of the bonds was studied by Fourier transform infrared (FTIR) spectrophotometry in a Nicolet 6700 spectrometer. The particle size distribution was determined by laser diffraction using a Malvern Mastersizer particle size analyzer in the range of 0.2−180 μm.

3. RESULTS

3.1. Comparison between Product Yields Obtained in Discontinuous and Continuous Modes. Figure 3 shows the effect of temperature (in the 500−700 °C range) on the yields of product fractions when HDPE was continuously fed into the reactor.

The waxes were found to be the fraction of highest yield from 500 to 650 °C. Their yield accounted for almost 70 wt % at 500 °C, and when added to the yield of the diesel fraction, the joint yield accounted for more than 90 wt %. The yield of waxes diminished as the temperature was raised, whereas the yields of gasoline and gas increased and that of diesel peaked at 30 wt % at 550 °C. For temperatures above 675 °C, the highest yield corresponded to the gas fraction.

A comparison between these results and those reported in the literature for fluidized bed reactors leads to the observation that the results obtained by Kaminsky et al.[22] at 600 °C are similar to those obtained in this study in the 650−700 °C range. This is explained by the longer residence time of the gases in the fluidized bed reactor (4 s, whereas in the conical spouted bed reactor, it is 0.01 s). Mastral et al.[26] pyrolyzed HDPE in a fluidized bed. Their gas yields at 650 and 700 °C were 18.8 and 56.3 wt %, respectively (the corresponding values in this study were 14.6 and 39.4 wt %). Jung et al.[29] used a fluidized bed to pyrolyze polypropylene (PP) and polyethylene (PE). At 660 and 700 °C, they obtained gas yields of 36.6 and 54.6 wt %, respectively (higher than those in this work), and yields for the total liquid fraction of 61.0 and 43.7 wt %, respectively (lower than those in this work).

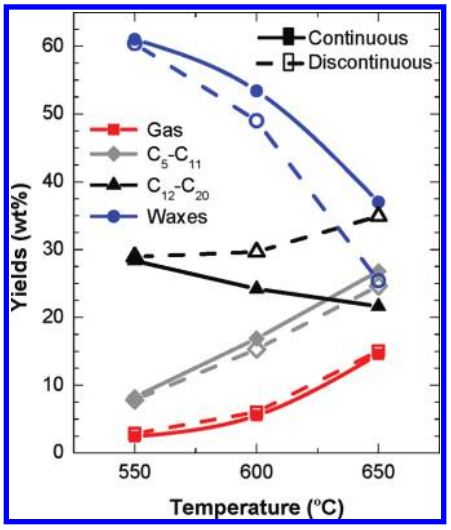

Figure 5. Comparison of the results for the yields of product fractions obtained in continuous and discontinuous modes.

Based on the results shown in Figure 3, it is concluded that thermal pyrolysis in continuous mode is a suitable process for obtaining high yields of waxes in the 500−550 °C range. Waxes are not of immediate commercial interest, but they are useful as feeds for refinery fluid catalytic cracking (FCC) units, to obtain fuels and C_2−C_4 olefins.[52,53]

Thermal pyrolysis above 550 °C gives rise to a wide product distribution, and consequently, a more detailed analysis is required to assess the products of possible commercial interest. Figure 4 shows the effect of temperature on the yields of the families of gas and gasoline fraction components. These results are of interest from a commercial point of view, given that high yields of C_2−C_4 olefins (37 wt % at 700 °C) and low aromatic contents in the gasoline fraction were obtained. The light alkanes are byproducts of low interest that are best used to supply energy to the process.

Figure 5 compares the yields of product fractions obtained in the pyrolysis of HDPE operating in discontinuous mode (dashed lines) with those obtained in continuous mode (solid lines) in the 550−650 °C range. Lower yields of waxes were observed when operating in discontinuous mode, whereas the yield of the diesel fraction was higher. This difference was found to be greater for higher temperatures. The yield of the gasoline fraction was slightly higher in continuous mode, and that of the gas fraction was similar.

The difference in the results observed between the two operating modes is due to the different compositions of the reaction media, as that in the continuous regime is constant. Operating in discontinuous mode, the high concentration of waxes (primary products) obtained at short reaction times enhances their cracking, which is explained by the higher yield of the diesel fraction, consisting of components with lower molecular weights than those in the waxes.

Although continuous operation facilitates the collection and analysis of the liquid, measures were taken to obtain reproducible results in both regimes. Hence, the differences are attributed to different compositions of the reaction media in the two regimes, which is relevant at these temperatures (above 600 °C) when secondary reactions are significant.

3.2. Individual Component Yields and Product Fraction Properties. The yields and compositions of the products were studied to analyze their capabilities as fuels and raw materials. They were grouped into four fractions: gas (C_{4-}), gasoline (C_5−C_{11}), diesel (C_{12}−C_{20}), and waxes (C_{21+}).

Table 1. Yields (wt %) of the Gas Fraction Components at Different Temperatures for Operation in Continuous Mode

	temperature				
component	500 °C	550 °C	600 °C	650 °C	700 °C
CH_4	0.03	0.02	0.16	1.02	0.91
C_2	0.15	0.30	1.33	4.20	17.86
ethane	0.07	0.05	0.08	0.07	0.04
ethylene	0.08	0.25	1.25	4.13	17.82
C_3	0.57	0.99	2.33	4.97	10.66
propane	0.06	0.13	0.26	0.50	0.21
propylene	0.51	0.86	2.07	4.47	10.45
C_4	0.75	1.11	1.72	4.37	10.01
C_{4-}	0.18	0.39	0.36	0.73	0.55
isobutane	0.02	0.23	0.03	0.05	0.05
n-butane	0.16	0.16	0.33	0.68	0.50
$C_{4=}$	0.58	0.72	1.36	3.64	9.46
1-butene	0.01	0.15	0.74	2.15	7.16
2-butene	0.15	0.17	0.18	0.38	0.20
isobutene	0.11	0.08	0.14	0.28	0.12
butadiene	0.31	0.32	0.30	0.83	1.98

3.2.1. Gas Fraction (C_{4-}). Table 1 shows the individual product yields for the components in the gas fraction, which increased with temperature in the 550−700 °C range. The yield of ethylene was found to increase in the most pronounced way, from 0.08 wt % at 500 °C to 17.82 wt % at 700 °C. This high increase in the yield of ethylene is in line with certain results in the literature obtained in fluidized bed reactors. Thus, at 700 °C, Mastral et al.[26] obtained 19.1 wt % of ethylene, and Jung et al.[29] obtained 18.2 wt %. Kaminsky et al.[22] obtained the markedly different value of 36.0 wt % for ethylene.

The yield of propylene also increased considerably as temperature was raised, from 0.51 wt % at 500 °C to 4.47 wt % at 650 °C and 10.45 wt % at 700 °C, and this increase was more tempered in the latter range than that for ethylene. Propylene is also the product reported in the literature to have the highest yield after ethylene. The yield of propylene accounted for 15.0 wt % at 700 °C in the study by Kaminsky et al.,[22] 15.6 wt % in that by Mastral et al.,[26] and 11.7 wt % in that by Jung et al.,[29] which are results similar to those obtained in this work.

The yield of C_4 olefins at 700 °C was high (9.46 wt %), similar to that of propylene, with a significant contribution of the yields of 1-butene (7.16 wt %) and, to a lesser extent, of butadiene (1.98 wt %). The yields of C_4 olefins followed a trend with temperature similar to that reported in the literature, and at 700 °C, they accounted for 1.5 wt % in the study by Kaminsky et al.,[22] 12.5 wt % in that by Mastral et al.,[26] and 5.6 wt % in that by Jung et al.[29]

The yield of C_{4-} alkanes increased slightly as temperature was increased, albeit in a less pronounced way than that of olefins. Methane had the highest yield, reaching a considerable value of 0.91 wt % at 700 °C. The individual yields for the remaining components were below 0.7 wt %. The yields obtained for C_{4-} alkanes in other studies were also lower than those of olefins, although the yield of methane obtained by Kaminsky et al.[22] at 700 °C was much higher than in our case. This difference could

dx.doi.org/10.1021/ie200186m |Ind. Eng. Chem. Res. 2011, 50, 6650–6659

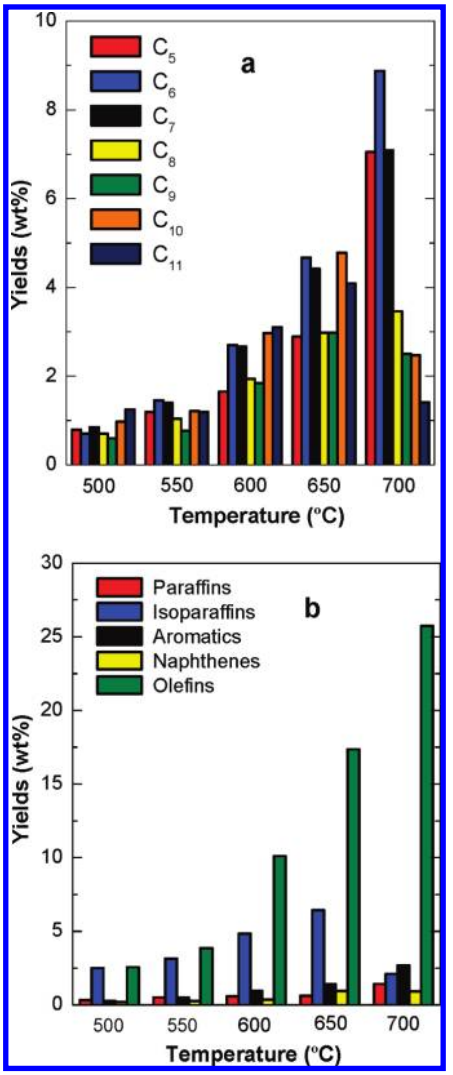

Figure 6. Effect of temperature on the yields of gasoline fraction components ordered according to (a) their carbon atom number and (b) the nature of their bonds. Continuous regime.

be explained by the defluidization problems of a fluidized bed working on a larger scale.

3.2.2. Gasoline Fraction (C_5−C_{11}). Figure 6 shows the effect of temperature on the gasoline fraction components (C_5−C_{11}), grouped according to their carbon atom numbers (a) and the nature of their bonds (b).

The yields of the components increased as temperature was raised. The distribution of the yields for components with different numbers of carbon atoms was found to be fairly uniform in the 500−650 °C range (Figure 6a). At 700 °C, the yields of C_5−C_7 components were higher, especially that of C_6.

An analysis of the nature of the bonds (Figure 6b) revealed that the highest yield was that of olefins, which increased considerably as temperature was raised. The yield of isoparaffins was also significant, although it increased with temperature to a lesser extent than that of olefins and even decreased at 700 °C. The yield of aromatic components also increased with temperature, but to a lesser extent than that of olefins. The yields of both linear paraffins and naphthenes were low and hardly varied with temperature.

The results obtained by Predel and Kaminsky[23] in a fluidized bed reactor concerning the total yield of C_5−C_{11} compounds

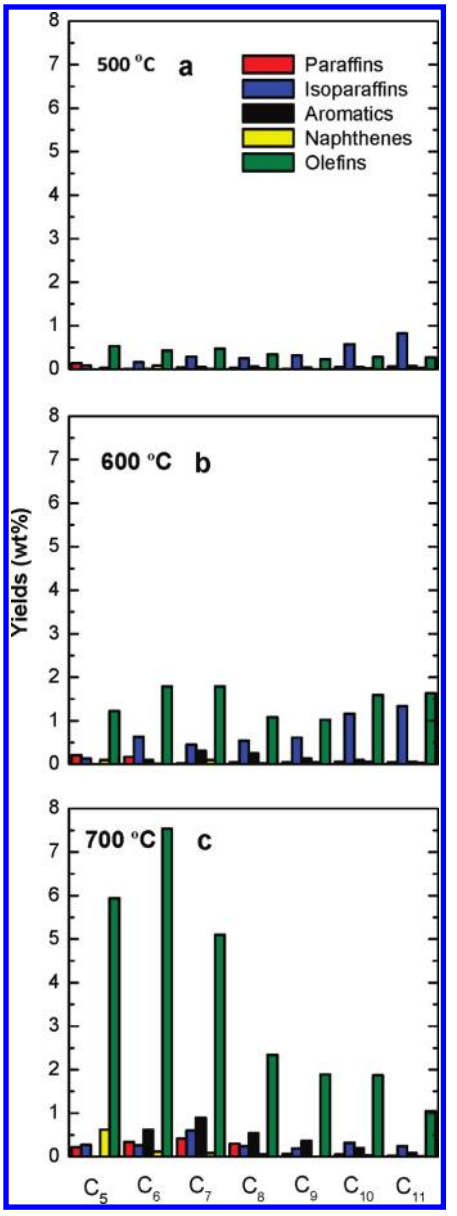

Figure 7. Yields for the different families in the gasoline fraction, grouped according to their carbon atom number, as a function of temperature: (a) 500, (b) 600, and (c) 700 °C. Continuous regime.

(5.8 wt % at 514 °C), the uniform distribution of individual yields, and the low yield of aromatic components are consistent with those obtained in this work, although those authors obtained mainly olefins at 514 °C, whereas in this work, olefins were obtained at higher temperatures.

The low yield of aromatic components is noteworthy, even at 700 °C, when compared with that obtained by Kaminsky et al.[22] at the same temperature (16 wt %) and Jung et al.[29] (9.1 wt % at 660 °C, with benzene and toluene as main products with yields of 2.8 and 2.4 wt %, respectively). This difference is associated with the lower residence time of the volatile products in the spouted bed reactor, where secondary reactions are minimized, specifically, the condensation of olefins to form aromatics.

The yields for family components grouped according to the number of carbon atoms are shown in Figure 7. Each graph corresponds to a given temperature. Figure 7a, corresponding to

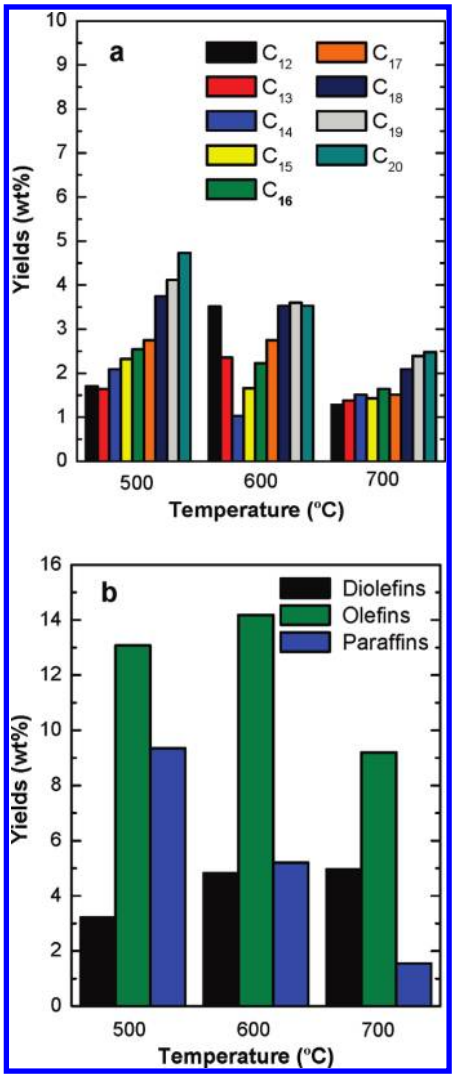

Figure 8. Effect of temperature on the yields of diesel fraction components, grouped by (a) their carbon atom number and (b) the nature of their bonds. Continuous regime.

500 °C, shows that the components with lower molecular weight were mainly olefins, whereas the heavier products were mainly isoparaffins. Figure 7b, for 600 °C, shows a rather uniform distribution for olefins. The yields of isoparaffins were higher as the molecular weight became higher. The yields of aromatic components were higher than at 500 °C and were mainly toluene and xylenes, although each one had a yield lower than 0.5 wt %. Figure 7c, corresponding to 700 °C, shows a distribution in which the higher yields are those for the light components (C_5−C_7), mainly olefins. It is worth noting that lower yields of isoparaffin components were obtained at 700 °C than at lower temperatures, whereas the yields of aromatics were already significant, especially those of benzene and toluene, with individual yields of around 1 wt %.

Table 2 lists the properties of the gasoline fractions obtained at different temperatures and the limits for commercial gasoline. The octane index (research octane number, RON) was higher for the fractions obtained at higher temperatures. The RON index values were lower than those for commercial gasoline (95 and 98 in the EU), and consequently, a good option would be to mix these gasoline fractions with other refinery streams of higher

Table 2. Properties of Commercial Interest for the Gasoline Fractions Obtained at Different Temperatures

temperature (°C)	octane index	olefins (%)	aromatics (%)	benzene (%)
500	81.4	43.6	4.7	0.2
550	79.5	46.8	6.0	0.4
600	84.1	59.9	5.7	0.6
650	85.2	64.8	5.3	0.5
700	86.3	78.3	8.2	1.9
required	95	<18	<35	<1

octane number whose aromatic and/or sulfur contents exceed standard requirements. In fact, the aromatic component concentration of the fractions obtained was well below the ceiling of 35% established by EU legislation.[54] Moreover, the absence of sulfur in these fractions is another positive aspect.

Furthermore, the gasoline fraction obtained at 700 °C was 1.9% benzene, whereas the limit for commercial gasoline is 1 wt %.

Nevertheless, the more serious drawback for the direct commercialization of these fractions is the high olefin concentration, which is limited to 18 wt % to avoid polymerization problems. The solution for adapting the gasoline fractions obtained to legal requirements would be mild hydrotreatment reforming in refineries.

3.2.3. Diesel Fraction (C_{12}−C_{20}). The effect of pyrolysis temperature on the composition of the diesel fraction is shown in Figure 8. The results are grouped according to their carbon atom number (Figure 8a) and type of bond (Figure 8b). In Figure 8b, unlike the classification carried out for the gasoline fraction, the components are arranged according to their diolefinic, olefinic, and paraffinic nature, given that the yields of naphthenes and aromatics were very low. The yields of the diolefin components were more significant than in the case of the gasoline fraction, which is also a common result reported in the literature on fluidized bed reactors.[23,25]

Figure 8a shows that the yield of the heaviest components decreased as temperature was increased and that the yield distribution obtained became more uniform. The yield of olefins was the highest one for the whole temperature range studied, peaking at 600 °C (Figure 8b). The yield of the diolefin components increased when increasing the temperature from 500 to 600 °C, whereas that of paraffins decreased linearly when temperature was raised.

The increase in the yield of diolefins with increasing temperature at the expense of a decrease in the yield of paraffins was also observed by Williams and Williams[55] in a fluidized bed reactor. Moreover, the paraffin/olefin/diolefin ratio obtained in this study at 500 °C (1.00:1.40:0.34) is of the same order as that obtained by Predel and Kaminsky[23] at 514 °C (1.00:2.20:0.25) and by Hernández et al.[56] at 500 °C (1.00:1.21:0.10). For the last authors, an increase in temperature also resulted in an increase in olefins, with the values of this ratio being 1.00:4.40:0.90 at 600 °C (1.00:2.70:0.90 in this work) and 1.00:4.00:1.30 at 700 °C (1.00:5.90:3.20 in this work).

The yields of components grouped according to their carbon atom numbers are displayed in Figure 9. Each graph corresponds to one temperature. It is observed in Figure 9a (corresponding to 500 °C) that the highest yields of olefins, diolefins, and paraffins were obtained for the components with the highest molecular weights. When the temperature was increased to 600 °C (Figure 9b), the

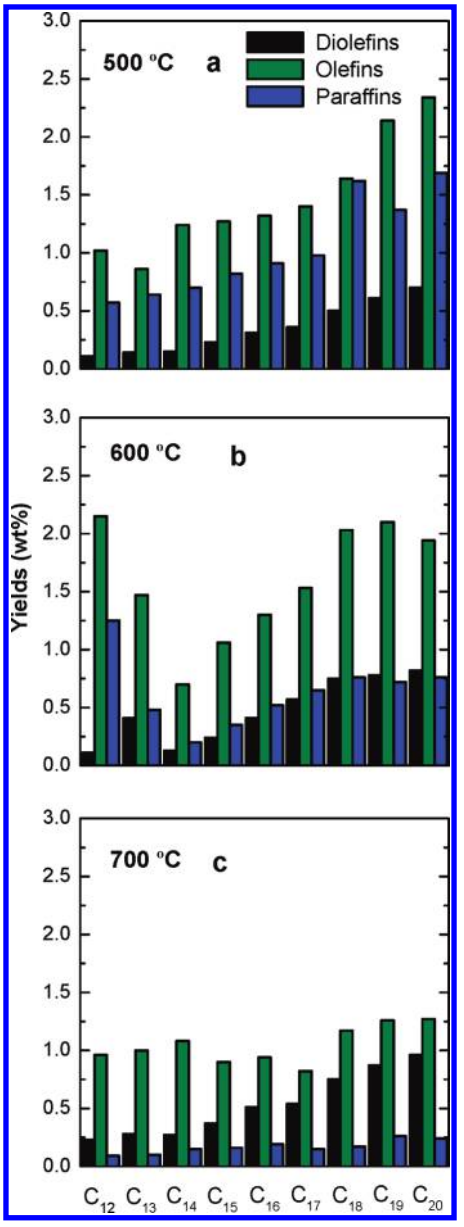

Figure 9. Yields of each of the families in the diesel fraction, grouped according to their carbon atom number, as a function of temperature: (a) 500, (b) 600, and (c) 700 °C. Continuous regime.

yields of C_{12} and C_{13} olefins and paraffins increased, whereas those of C_{19} and C_{20} olefins and paraffins decreased. An increase in temperature to 700 °C (Figure 9c) resulted in a lower yield for the diesel fraction and a uniform distribution for the yields of olefins with different numbers of carbon atoms, whereas the yields obtained in the case of paraffins and diolefins were higher as the number of carbon atoms increased. These trends for the effect of temperature are consistent with the results obtained by Hernández et al.[56]

The cetane index of this fraction mixture was determined from the yields of the individual components, following the standard indicated by the EU, ASTM D4737. Table 3 lists the cetane index and other properties of the $C_{12}-C_{20}$ fraction, together with EU requirements (Directive 2009/30/EC, effective as of Jan 1, 2009).[54]

Based on the aforementioned results, the yield of the diesel fraction is high (30 wt % at 550 °C), and its properties are encouraging from a commercial point of view.

Table 3. Properties of the Diesel Fraction Obtained in the Continuous Regime and Requirements for Commercial Diesel (A) According to Current EU Regulations

property	500 °C	600 °C	700 °C	required
cetane index	85.4	85.8	84.4	>46
density at 15 °C ($kg\ m^{-3}$)	785	784	786	820−845
PAH content	insignificant	insignificant	insignificant	<11%
sulfur content (ppm)	insignificant	insignificant	insignificant	<10 ppm
distillation curve				
65 wt %	314	308	307	>250 °C
85 wt %	326	325	325	<350 °C
95 wt %	328	328	327	<360 °C

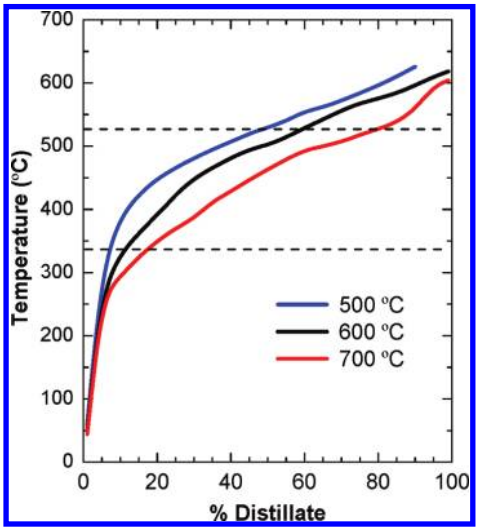

Figure 10. Simulated distillation curves for the wax fractions obtained at different temperatures. Continuous regime.

3.2.4. Waxes (C_{21+}). The simulated distillation curves corresponding to the waxes obtained at different temperatures are shown in Figure 10. It is observed that part of the gasoline and diesel fraction components dissolved in the waxes. Based on the paraffin standards used, two fractions were quantified (separated by dashed lines in Figure 10): (i) light waxes, the $C_{21}-C_{40}$ fraction, corresponding to compounds with boiling points in the 343−525 °C range, and (ii) heavy waxes (the remaining waxes). It should be noted that the temperature of 343 °C is commonly considered to be the minimum temperature to define the HCO (heavy cycle oil) fraction. Predel and Kaminsky[23] delimited a light wax fraction in the 300−500 °C range (corresponding to $C_{17}-C_{36}$ compounds). It was observed that, as the reaction temperature was raised, the content of the light fraction compounds (C_{20-}) dissolved in the waxes increased: 7, 12, and 19 wt % for 500, 600, and 700 °C, respectively. Furthermore, when the temperature was increased, the average molecular weight of the waxes was lower, although compounds that were heavier than the heaviest standard that can be measured accurately (C_{64}) were detected by liquid chromatography. The ratios of light wax to heavy wax by mass were found to be 0.5, 1.1, and 3.0 at 500, 600, and 700 °C, respectively.

Figure 11 shows the molecular weight distributions of the waxes obtained at different temperatures by liquid chromatography

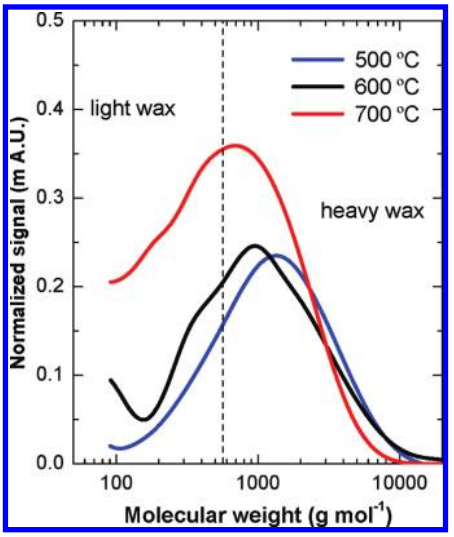

Figure 11. Molecular weight distributions (determined by GPC) of the waxes obtained at different temperatures. Continuous regime.

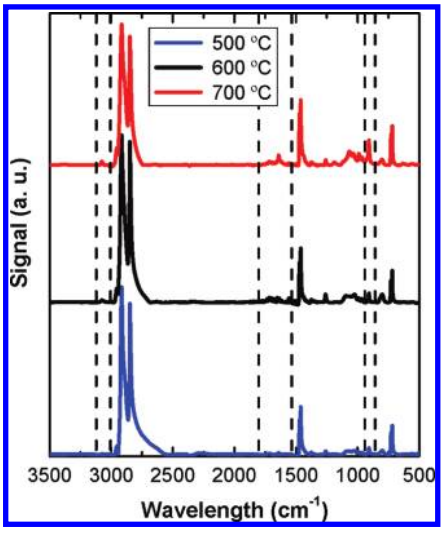

Figure 12. FTIR spectra of the waxes obtained at different temperatures. Continuous regime.

analysis. The results confirm the aforementioned effect; that is, an increase in reaction temperature involved the production of lighter waxes. Moreover, this allows the information concerning the distribution of component boiling points to be improved, which is important for assessing the compatibility of these waxes with the usual feed in a refinery unit (such as an FCC or hydrocracking unit).

The average molecular weight by mass varied from 1558 Da for the waxes obtained at 500 °C to 1247 Da for those obtained at 700 °C. Assuming hydrocarbon chains made of $-CH_2-$ groups (as indicated by the results identifying light waxes carried out by means of MS and FTIR spectrophotometry), these results would correspond, on average, to chains of 112 carbon atoms for the waxes obtained at 500 °C and 89 for those obtained at 700 °C.

These values of average molecular weight are higher than those obtained by Williams and Williams[55] (736−742 Da), which is explained by the shorter residence time of the volatiles in the spouted bed reactor compared to the fluidized bed and, consequently, the mild cracking of the waxes formed as primary products.

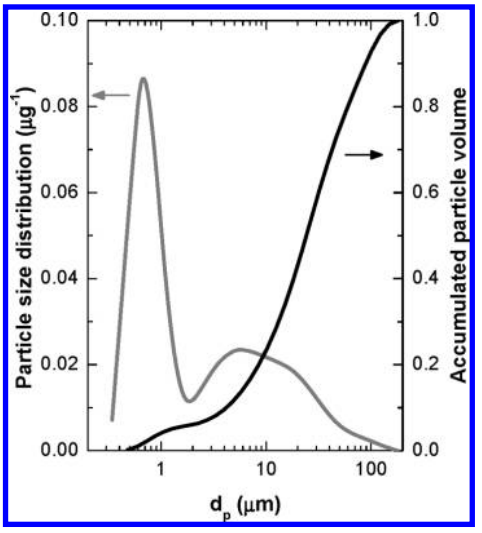

Figure 13. Particle size distribution of the waxes obtained at 500 °C. Continuous regime.

As is observed in the FTIR spectra of the waxes (Figure 12), the symmetric and asymmetric bands characteristic of C−H bonds corresponding to $-CH_2-$ groups at 2855 and 2920 cm^{-1} are similar to the bands of the same group of commercial waxes.[57,58] Likewise, the double peak at 725 cm^{-1} matches the skeletal vibration of these peaks. Two shoulders were observed at 2960 and 2900 cm^{-1} that correspond to the $-CH_3$ terminal groups, although they are more noticeable in the case of commercial waxes. This confirms that the waxes obtained in HDPE pyrolysis have fewer branched chains than commercial waxes. Other bands were observed at 1386 and 1471 cm^{-1}, corresponding to aliphatic chains, due to the bending vibrations of methyl and methylene groups. The bands at 1646 and 1725 cm^{-1} were caused by the stretching of C═C bonds, which confirms the presence of olefins.

Another significant difference from the commercial waxes lies in the more olefinic nature of the waxes obtained in HDPE pyrolysis, which is explained by the radical degradation mechanism of HDPE pyrolysis. This olefinic nature is corroborated by the bands at 910 and 995 cm^{-1}, corresponding to R—$CH{=}CH_2$.[58] The olefinic nature is clearly observed in the FTIR results for the waxes obtained at the highest temperature.

Hardly any peaks were detected corresponding to bands denoting the presence of aromatic components at 1500 and 3000−3100 cm^{-1}.[55] Nevertheless, a peak appeared between 3000 and 3100 cm^{-1} for the waxes obtained at 700 °C, even though it was very small.

The particle size distribution of the waxes obtained at 500 °C is shown in Figure 13. The prevailing size was 0.7 μm, although the main range (more than 80% of the sample volume) was between 15 and 80 μm.

The higher heating value of the waxes increased as the pyrolysis temperature was raised, with values of 35.6, 44.1, and 45.4 MJ kg^{-1} for 500, 600, and 700 °C, respectively, which may be attributed to the lower average molecular weight mentioned above.

CONCLUSIONS

The conical spouted bed reactor performs well for polyolefin pyrolysis carried out in continuous mode. The cyclic movement of the particles facilitates their uniform coating with fused plastic,

improving the rates of heat and mass transfer between the phases. Moreover, the short residence time of the volatiles minimizes the formation of byproducts (methane and polyaromatic hydrocarbons). Comparing the results with those obtained by operating in discontinuous mode shows that the yields of gases were similar and the yields of waxes and the gasoline fraction were higher in continuous mode, at the expense of a decrease in the yield of the diesel fraction.

The polyolefin pyrolysis process is versatile in the 500−700 °C range. When feeding HDPE, the yield of waxes (C_{21+}) was found to account for 67 wt % at 500 °C and to decrease to 12 wt % in this range. An increase in temperature was found to result in an increase in the gases (C_{4-}) and gasoline fraction (C_5−C_{11}), which accounted for 39 and 33 wt %, respectively, at 700 °C, whereas the yield of diesel (C_{12}−C_{20}) decreased (16 wt % at 700 °C). Consequently, the conical spouted bed is an excellent technology for obtaining waxes at low temperatures (500 °C) without defluidization problems, making the resulting waxes a suitable feed for FCC units. On the other hand, operation at high temperature (700 °C) is promising for obtaining gasoline (33 wt % with a significant content of C_5−C_7 olefins), together with a high yield of C_2−C_4 olefins (37 wt %).

AUTHOR INFORMATION

Corresponding Author

*Tel.: (+34) 946 015414. Fax: (+34) 946 013500. E-mail: gorka.elordi@ehu.es.

ACKNOWLEDGMENT

This study was carried out with the financial support of the Ministry of Science and Education of the Spanish Government (Project CTQ2007-61167) and the Basque Government (Project GIC07/24-IT-220-07) and with a bursary for University Teacher Training (AP2005-3123).

REFERENCES

(1) Aguado, J.; Serrano, D. P. *Feedstock Recycling of Plastic Wastes*; The Royal Society of Chemistry: Cambridge, U.K., 1999.

(2) Scheirs, J.; Kaminsky, W. *Feedstock Recycling and Pyrolysis of Waste Plastics, Converting Waste Plastics into Diesel and Other Fuels*, John Wiley and Sons: Chichester, U.K., 2006.

(3) Al-Salem, A. M.; Lettieri, P.; Baeyens, J. Recycling and Recovery Routes of Plastic Solid Waste (PSW): A Review. *Waste Manage.* **2009**, *29*, 2625–2643.

(4) Al-Salem, A. M.; Lettieri, P.; Baeyens, J. The Valorization of Plastic Solid Waste (PSW) by Primary to Quaternary Routes: From Reuse to Energy and Chemicals. *Prog. Energy Combust. Sci.* **2010**, *36*, 103–129.

(5) Siddiqui, M. N. Conversion of Hazardous Plastic Wastes into Useful Chemical Products. *J. Hazard. Mater.* **2009**, *167*, 728–735.

(6) Ueno, T.; Nakashima, E.; Takeda, K. Quantitative Analysis of Random Scission and Chain-End Scission in the Thermal Degradation of Polyethylene. *Polym. Degrad. Stabil.* **2010**, *95*, 1862–1869.

(7) Encinar, J. M.; González, J. F. Pyrolysis of Synthetic Polymers and Plastic Wastes. Kinetic Study. *Fuel Process. Technol.* **2008**, *89*, 678–686.

(8) Al-Salem, A. M.; Lettieri, P. Kinetic Study of High Density Polyethylene (HDPE) Pyrolysis. *Chem. Eng. Res. Des.* **2010**, *88*, 1599–1606.

(9) Hujuri, U.; Ghoshal, A. K.; Gumma, S. Temperature-Dependent Pyrolytic Product Evolution Profile for Low-Density Polyethylene from Gas Chromatographic Study. *Waste Manage.* **2010**, *30*, 814–820.

(10) Marcilla, A.; Beltrán, M.; Hernández, F.; Navarro, R. HZSM5 and HUSY Deactivation During the Catalytic Pyrolysis of Polyethylene. *Appl. Catal. A: Gen.* **2004**, *278*, 37–43.

(11) Marcilla, A.; Beltrán, M.; Navarro, R. Thermal and Catalytic Pyrolysis of Polyethylene over HZSM5 and HUSY Zeolites in a Batch Reactor under Dynamic Conditions. *Appl. Catal. B: Environ.* **2009**, *86*, 78–86.

(12) Serrano, D. P.; Aguado, J.; Escola, J. M.; Garagorri, E.; Rodríguez, J. M.; Morselli, L.; Palazzi, G.; Orsi, R. Feedstock Recycling of Agriculture Plastic Film Wastes by Catalytic Cracking. *Appl. Catal. B: Environ.* **2004**, *49*, 257–265.

(13) Achilias, D. S.; Roupakias, C.; Megalokonomos, P.; Lappas, A. A.; Antonakou, E. V. Chemical Recycling of Plastic Wastes Made from Polyethylene (LDPE and HDPE) and Polypropylene (PP). *J. Hazard. Mater.* **2007**, *149*, 536–542.

(14) Chaianansutcharit, S.; Katsutath, R.; Chaisuwan, A.; Bhaskar, T.; Nigo, A.; Muto, A.; Sakata, Y. Catalytic Degradation of Polyolefins over Hexagonal Mesoporous Silica: Effect of Aluminum Addition. *J. Anal. Appl. Pyrolysis* **2007**, *80*, 360–368.

(15) Della Zassa, M.; Favero, M.; Canu, P. Two-steps Selective Thermal Depolymerization of Polyethylene. 1: Feasibility and Effect of Devolatilization Heating Policy. *J. Anal. Appl. Pyrolysis* **2010**, *87*, 248–255.

(16) Aguado, J.; Serrano, D. P.; Escola, J. M. Fuels from Waste Plastics by Thermal and Catalytic Processes: A Review. *Ind. Eng. Chem. Res.* **2008**, *47*, 7982–7992.

(17) Serrano, D. P.; Aguado, J.; Escola, J. M.; Garagorri, E. Conversion of Low Density Polyethylene into Petrochemical Feedstocks Using a Continuous Screw Kiln Reactor. *J. Anal. Appl. Pyrolysis* **2001**, *58*−*59*, 789–801.

(18) Aguado, J.; Serrano, D. P.; Escola, J. M.; Garagorri, E. Catalytic Conversion of Low-Density Polyethylene Using a Continuous Screw Kiln Reactor. *Catal. Today* **2002**, *75*, 257–262.

(19) Serrano, D. P.; Aguado, J.; Escola, J. M.; Garagorri, E. Performance of a Continuous Screw Kiln Reactor for the Thermal and Catalytic Conversion of Polyethylene−Lubricating Oil Base Mixtures. *Appl. Catal. B: Environ.* **2003**, *44*, 95–105.

(20) Miskolczi, N.; Angyal, A.; Bartha, L.; Valkai, I. Fuels by Pyrolysis of Waste Plastics from Agricultural and Packaging Sectors in a Pilot Scale Reactor. *Fuel Process. Technol.* **2009**, *90*, 1032–1040.

(21) Kaminsky, W. Chemical Recycling of Mixed Plastics by Pyrolysis. *Adv. Polym. Technol.* **1995**, *14*, 337–344.

(22) Kaminsky, W.; Schlesselmann, B.; Simon, C. Olefins from Polyolefins and Mixed Plastics by Pyrolysis. *J. Anal. Appl. Pyrolysis* **1995**, *32*, 19–27.

(23) Predel, M.; Kaminsky, W. Pyrolysis of Mixed Polyolefins in a Fluidised-Bed Reactor and on a Pyro-GC/MS to Yield Aliphatic Waxes. *Polym. Degrad. Stabil.* **2000**, *70*, 373–385.

(24) Mastellone, M. L.; Perugini, F.; Ponte, U.; Arena, U. Fluidized Bed Pyrolysis of a Recycled Polyethylene. *Polym. Degrad. Stabil.* **2002**, *76*, 479–487.

(25) Bagri, R.; Williams, P. T. Catalytic Pyrolysis of Polyethylene. *J. Anal. Appl. Pyrolysis* **2002**, *63*, 29–41.

(26) Mastral, F. J.; Esperanza, E.; García, P.; Juste, M. Pyrolysis of High-Density Polyethylene in a Fluidised Bed Reactor. Influence of the Temperature and Residence Time. *J. Anal. Appl. Pyrolysis* **2002**, *63*, 1–15.

(27) Lee, C. G.; Cho, Y. J.; Song, P. S.; Kang, Y.; Kim, J. S.; Choi, M. J. Effects of Temperature Distribution on the Catalytic Pyrolysis of Polystyrene Waste in a Swirling Fluidized-Bed Reactor. *Catal. Today* **2003**, *79*−*80*, 453–464.

(28) Marcilla, A.; Hernández, M. R.; García, A. N. Degradation of LDPE/VGO Mixtures to Fuels Using a FCC Equilibrium Catalyst in a Sand Fluidized Bed Reactor. *Appl. Catal. A: Gen.* **2008**, *341*, 181–191.

(29) Jung, S.; Cho, M.; Kang, B.; Kim, J. Pyrolysis of a Fraction of Waste Polypropylene and Polyethylene for the Recovery of BTX Aromatics Using a Fluidized Bed Reactor. *Fuel Process. Technol.* **2010**, *91*, 277–284.

(30) Martinez, L.; Aguado, A.; Moral, A.; Irusta, R. Fluidized Bed Pyrolysis of HDPE: A Study of the Influence of Operating Variables and

the Main Fluidynamic Parameters on the Composition and Production of Gases. *Fuel Process. Technol.* **2011**, *92*, 221–228.
(31) Aguado, R.; Olazar, M.; Gaisán, B.; Prieto, R.; Bilbao, J. Kinetic Study of Polyolefins Pyrolysis in a Conical Spouted Bed Reactor. *Ind. Eng. Chem. Res.* **2002**, *41*, 4559–4566.
(32) Aguado, R.; Olazar, M.; San José, M. J.; Gaisán, B.; Bilbao, J. Wax Formation in the Pyrolysis of Polyolefins in a Conical Spouted Bed Reactor. *Energy Fuels* **2002**, *16*, 1429–1437.
(33) Elordi, G.; Olazar, M.; Lopez, G.; Amutio, M.; Artetxe, M.; Aguado, R.; Bilbao, J. Catalytic Pyrolysis of HDPE in Continuous Mode over Zeolite Catalysts in a Conical Spouted Bed Reactor. *J. Anal. Appl. Pyrolysis* **2009**, *85*, 345–351.
(34) Elordi, G.; Lopez, G.; Olazar, M.; Aguado, R.; Bilbao, J. Product Distribution Modelling in the Thermal Pyrolysis of High Density Polyethylene. *J. Hazard. Mater.* **2007**, *144*, 708–714.
(35) Silveira da Rosa, G.; dos Santos Rocha, S. C. Effect of Process Conditions on Particle Growth for Spouted Bed Coating of Urea. *Chem. Eng. Process. Process Intens.* **2010**, *49*, 836–842.
(36) Bilbao, J.; Olazar, M.; Romero, A.; Arandes, J. M. Design and Operation of a Jet Spouted Bed Reactor with Continuous Catalyst Feed in the Benzyl Alcohol Polymerization. *Ind. Eng. Chem. Res.* **1987**, *26*, 1297–1304.
(37) Olazar, M.; San José, M. J.; Zabala, G.; Bilbao, J. A New Reactor in Jet Spouted Bed Regime for Catalytic Polymerizations. *Chem. Eng. Sci.* **1994**, *49*, 4579–4588.
(38) Lin, Y. H.; Yang, M. H. Tertiary Recycling of Polyethylene Waste by Fluidised-Bed Reactions in the Presence of Various Cracking Catalysts. *J. Anal. Appl. Pyrolysis* **2008**, *83*, 101–109.
(39) San José, M. J.; Olazar, M.; Peñas, F. J.; Arandes, J. M.; Bilbao, J. Correlation for Calculation of the Gas Dispersion Coefficient in Conical Spouted Beds. *Chem. Eng. Sci.* **1995**, *50*, 2161–2172.
(40) Olazar, M.; San José, M. J.; Peñas, F. J.; Aguayo, A. T.; Arandes, J. M.; Bilbao, J. A Simplified Model for Gas Flow in Conical Spouted Beds. *Chem. Eng. J.* **1995**, *56*, 19–26.
(41) Olazar, M.; San José, M. J.; Peñas, F. J.; Aguayo, A. T.; Bilbao, J. The Stability and Hydrodynamics of Conical Spouted Beds with Binary Mixtures. *Ind. Eng. Chem. Res.* **1993**, *32*, 2826–2834.
(42) San José, M. J.; Olazar, M.; Peñas, F. J.; Bilbao, J. Segregation in Conical Spouted Beds with Binary and Tertiary Mixtures of Equidensity Spherical Particles. *Ind. Eng. Chem. Res.* **1994**, *33*, 1838–1844.
(43) Olazar, M.; San José, M. J.; Aguayo, A. T.; Arandes, J. M.; Bilbao, J. Stable Operation Conditions for Gas−Solid Contact Regimes in Conical Spouted Beds. *Ind. Eng. Chem. Res.* **1992**, *31*, 1784–1791.
(44) Olazar, M.; San José, M. J.; Aguayo, A. T.; Arandes, J. M.; Bilbao, J. Design Factors of Conical Spouted Beds and Jet Spouted Beds. *Ind. Eng. Chem. Res.* **1993**, *32*, 1245–1250.
(45) Olazar, M.; San José, M. J.; Alvarez, S.; Morales, A.; Bilbao, J. Measurement of Particle Velocities in Conical Spouted Beds Using an Optical Fiber Probe. *Ind. Eng. Chem. Res.* **1998**, *37*, 4520–4527.
(46) Olazar, M.; San José, M. J.; Alvarez, S.; Morales, A.; Bilbao, J. Design of Conical Spouted Beds for the Handling of Low Density Solids. *Ind. Eng. Chem. Res.* **2004**, *43*, 655–661.
(47) San José, M. J.; Olazar, M.; Alvarez, S.; Bilbao, J. Local Bed Voidage in Conical Spouted Beds. *Ind. Eng. Chem. Res.* **1998**, *37*, 2553–2558.
(48) San José, M. J.; Olazar, M.; Alvarez, S.; Izquierdo, M. A.; Bilbao, J. Solid Cross-Flow into the Spout and Particle Trajectories in Conical Spouted Beds. *Chem. Eng. Sci.* **1998**, *53*, 3561–3570.
(49) San José, M. J.; Olazar, M.; Alvarez, S.; Morales, A.; Bilbao, J. Spout and Fountain Geometry in Conical Spouted Beds Consisting of Solids of Varying Density. *Ind. Eng. Chem. Res.* **2005**, *44*, 193–200.
(50) San José, M. J.; Olazar, M.; Alvarez, S.; Morales, A.; Bilbao, J. Local Porosity in Conical Spouted Beds Consisting of Solids of Varying Density. *Chem. Eng. Sci.* **2005**, *60*, 2017–2025.
(51) San José, M. J.; Alvarez, S.; Ortiz de Salazar, A.; Olazar, M.; Bilbao, J. Operating Conditions of Conical Spouted Beds with a Draft Tube. Effect of the Diameter of the Draft Tube and of the Height of Entrainment Zone. *Ind. Eng. Chem. Res.* **2007**, *46*, 2877–2884.
(52) Arandes, J. M.; Torre, I.; Castaño, P.; Olazar, M.; Bilbao, J. Catalytic Cracking of Waxes Produced by Polyolefins Fast Pyrolysis. *Energy Fuels* **2007**, *21*, 561–569.
(53) Arandes, J. M.; Torre, I.; Azkoiti, M. J.; Castaño, P.; Bilbao, J.; de Lasa, H. Effect of Catalyst Properties on the Cracking of Polypropylene Pyrolysis Waxes under FCC Conditions. *Catal. Today* **2008**, *133−135*, 413–419.
(54) Directive 2009/30/EC of the European Parliament and of the Council of 23 April 2009. *Off. J. Eur. Union* **2009**, *5.06.2009*, L140/88−L140/113.
(55) Williams, P. T.; Williams, E. A. Fluidised Bed Pyrolysis of Low Density Polyethylene to Produce Petrochemical Feedstock. *J. Anal. Appl. Pyrolysis* **1999**, *51*, 107–126.
(56) Hernández, M. R.; García, A. N.; Marcilla, A. Catalytic Flash Pyrolysis of HDPE in a Fluidized Bed Reactor for Recovery of Fuel-like Hydrocarbons. *J. Anal. Appl. Pyrolysis* **2007**, *78*, 272–281.
(57) Vogel, A. *Vogel's Textbook of Practical Organic Chemistry*; Longman: New York, 1981.
(58) Chaala, A.; Darmstadt, H.; Roy, C. Vacuum Pyrolysis of Electric Cable Wastes. *J. Anal. Appl. Pyrolysis* **1997**, *39*, 79–96.